International Journal of Mechanical, Industrial and Aerospace Sciences
ISSN: 2517-9950
Vol:9, No:12, 2015

Conceptual Design of Unmanned Aerial Targets

M. Adamski, J. Cwiklak

***Abstract*—**The contemporary battlefield creates a demand for more costly and highly advanced munitions. Training personnel responsible for operations as well as immediate execution of combat tasks which engage real asset is unrealistic and economically not feasible. Owing to a wide array of exploited simulators and various types of imitators, it is possible to reduce the costs. One of the effective elements of training, which can be applied in the training of all service branches, is imitator of aerial targets. This research serves as an introduction to the commencement of design analysis over a real aerial target imitator. Within the project, the basic aerodynamic calculations were made, which enabled to determine its geometry, design layout, performance as well as mass balance of individual components. The conducted calculations of the parameters of flight characteristics come closer to the real performance of such Unmanned Aerial Vehicles.

***Keywords*—**Aerial target, aerodynamics, imitator, performance.

I. Introduction

THE use of more costly and technologically advanced weapons and equipment in contemporary armed forces creates a demand to modify the training process of military personnel. Troops should practise in conditions which are as close as possible to real conditions in theatre. The procurement and maintenance costs of modern armaments are steadily growing. One of the ways of reducing these expenditures is to rationalize the training expenses. Owing to a common application of simulators and various types of imitators, it is possible to lower the costs, both in the training of land forces, crews of Unmanned Aerial Vehicles, naval ships and the air defence. One of the most effective training elements, exploited in the above-mentioned services, are imitators of aerial targets.

The low cost of manufacturing an imitator makes its loss in combat operations not so painful as in the case of other aerial vehicles. The cost of shooting down such an imitator may prove more expensive than the value of the imitator itself. Imitators of aerial targets may successfully be used in deceiving the enemy air defence. Simulating air assaults by means of the imitators may lead to lowering the enemy combat readiness, due to the necessity of engaging its elements to counteract a potential threat [4]. The capabilities of using imitators of aerial targets also include airstrikes. An imitator equipped with munitions is a target which is dangerous and difficult to eliminate. The cost of obtaining it is considerably lower than the value of potential targets which may be destroyed. A broad spectrum of applying this sort of unmanned vehicles and a relatively low manufacture cost, compared with other aerial vehicles, renders exploitation of suchlike drones justifiable, in the armed forces [1].

M. Adamski and J. Cwiklak are with the Polish Air Force Academy, Dywizjonu 303/35, 08-530 Deblin, Poland (corresponding author: M. Adamski; phone: +48 815517423; e-mail: j.cwiklak@wsosp.pl, terazen@wp.pl).

II. Project Assumptions

A preliminary design of an Unmanned Aerial Vehicle should include tactical, technical, technological and exploitation needs. However, meeting all these requirements is often connected with a great deal of difficulties, since they are often contradictory and in many cases impossible to combine [9].

Basic geometrical dimensions:
- wing span – $l = 3$ m;
- length – $l_k = 2.60$ m;
- maximum length of fuselage – 0.4 m;
- maximum height of fuselage – 0.4 m;
- length of root chord – b_n=0.56 m;
- length of tip chord – b_k=0.2 m;
- wing surface area- S=1.14 m^2.

Other assumptions:
- cruising speed -350 km/h;
- propulsion – jet engine;
- ceiling – 6000 m;
- Maximum Take-off Mass – 90 kg.

Judging by the development tendencies of the exploited imitators (measurements, types of propulsion, tasks and the like), basic geometrical dimensions and aerodynamics as well as the initial assumptions for flight parameters were specified [2].

III. Model Mass

The knowledge of particular components and other major elements of an aircraft, as well as the assumed payload, which add to the weight during a flight, is essential to determine the location of the centre of gravity, and to establish its approximate weight [3].

Notation used in the calculations:
- m_s – mass of wing;
- m_{to} – aircraft take-off mass;
- n_A – coefficient of maximum permissible payload;
- υ – factor of safety;
- Λ – aspect ratio;
- g_o – relative thickness of root airfoil;
- χ – wing sweep of the quarter chord line (0.25);
- S – lift surface;
- τ – taper ratio;
- φ – load factor;
- Δp_k – maximum pressure differential limit in fuselage;
- V_{cruise} – cruising speed;
- q_k – unit mass of fuselage;

- S_k – fuselage front surface;
- S_{omk} –fuselage area of airflow;
- D_k - hydraulic diameter of fuselage.

On the basis of the calculations, it is assumed that the mass of the wing equals $m_s \approx 6$ kg and mass of fuselage is assumed to equal $m_k \approx 9$ kg**.** Due to the use of V-tail, the surface area of an elevator unit and a vertical tail unit have been replaced with projections of these planes on the horizontal and vertical plane, respectively. Taking into account the above results, the mass of tail is assumed to be equal to $m_{hv} \approx 2.2$ kg.

TABLE I
LISTING OF MASSES

Lp.	Component	Mass [kg]	Distance [m]
1	Radar reflector	$m_1 = 1$	$x_1 = 0.127$
2	Cargo area	$m_2 = 3$	$x_2 = 0.379$
3	Autopilot+GPS+INS	$m_3 = 6$	$x_3 = 0.81$
4	Cargo area	$m_4 = 7$	$x_4 = 0.81$
5	MDI	$m_5 = 5.89$	$x_5 = 1.26$
6	Fuselage	$m_6 = 9$	$x_6 = 1.26$
7	Fuel tank	$m_7 = 31.5$	$x_7 = 1.426$
8	Wing	$m_8 = 6$	$x_8 = 1.438$
9	Pylons	$m_9 = 2$	$x_9 = 1.438$
10	Parachute	$m_{10} = 5$	$x_{10} = 1.9$
11	Batteries	$m_{11} = 3$	$x_{11} = 1.867$
12	Steering system	$m_{12} = 1.3$	$x_{12} = 2.1$
13	Flare dispenser	$m_{13} = 3$	$x_{13} = 2.2$
14	Control surfaces	$m_{14} = 2.2$	$x_{14} = 2.33$
15	Engine	$m_{15} = 4.1$	$x_{15} = 2.33$
	TOTAL $\sum$	$m_{to} = 90$	$x_{sa} = 21.472$

On the basis of the data listed in Table I and (1), it is possible to calculate the position of the centre of gravity of the designed imitator of an aerial target.

$$x_{sa} = \sum_{n=1}^{n=15} \frac{x_n \cdot m_n}{m_{to}} \ [m] \tag{1}$$

The centre of gravity against the longitudinal axis is away from the nose edge of the designed aerial vehicle by x_{sa}=1.41m, which is included within 0.25-0.33 mean aerodynamic chord of the wing.

IV. AIRFOIL

Taking into account the geometric data and the analysis of available aerial vehicles of this type, the value of Reynolds number has been calculated, which is equal to the assumed minimum steady flight speed of 100 km/h (at low levels) [2]:

$$R_e \frac{Vsl \ \times b_{sa}}{V_0} \tag{2}$$

where: Re – Reynolds number; V_{sl} =27.7 m/s - velocity; b_{sa} =0.4084 m – length of mean aerodynamic chord; ν_0 =0.0000143 m^2/s – coefficient of kinematic viscosity. For the above data $Re \approx 0.8 \cdot 10^6$**.**

Taking advantage of the X-foil-5 programme, from the database of the available airfoils, the nine 6-series low-drag airfoils were selected. They were next subject to simulation with the panel method. The obtained characteristics were z=f(α) and cx=f(α) for Reynolds number $Re=0.8 \cdot 10^6$.

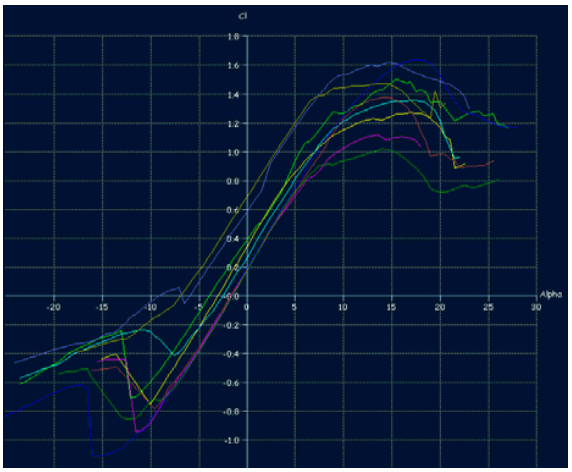

Fig. 1 Characteristics of selected airfoils c_z=f(α)

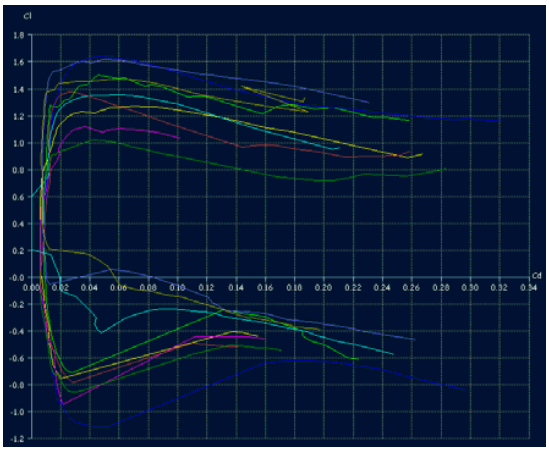

Fig. 2 Characteristics of selected airfoils c_x=f(α)

On the basis of the obtained graphs, the airfoil NACA $63_{(2)}215B$ was selected, which is characterized by low drag and a wide range of useful angles of attack.

Using the data from the X-foil 5 programme, for Reynolds number $0.8 \cdot 10^6$, the following airfoil characteristics of c_z=f(α) and c_x=f(α) have been generated:

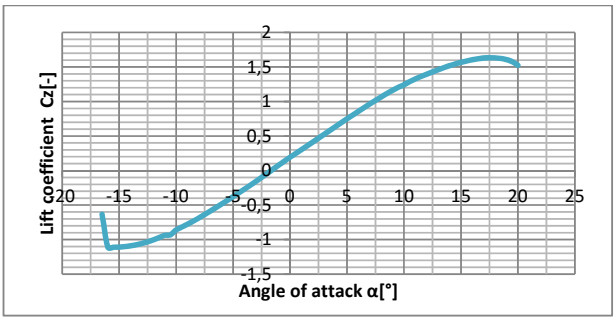

Fig. 3 Dependence of the lift coefficient on the angle of attack

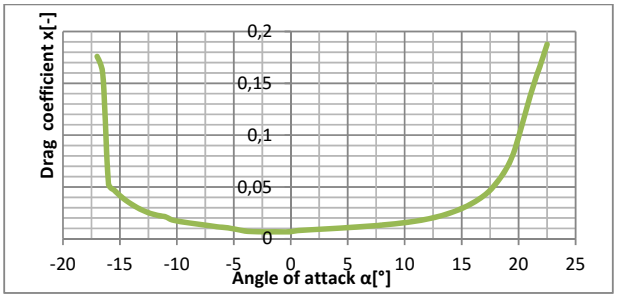

Fig. 4 Dependence of the drag coefficient on the angle of attack

V. Determining Drag Coefficient of Particular Elements

The main element which affects the change in drag, depending upon the lift, is a three-dimensional airflow of the wing. In the subsonic range, wing drag can be shown depending upon the drag which occurs in two-dimensional flow and drag induced as follows [3]:

$$c_{xs} = c_{xmin} + \frac{c_z^2}{\pi \cdot \Lambda_e} \tag{3}$$

Summing up the particular values and using the formula for aspect ratio, value of the aspect ratio Λ_e=7.178 was obtained, which entails the value of the wing drag coefficient c_{xs}=0.0788**.**

Fuselage drag coefficient, similarly to the wing drag, for currently used well-shaped fuselages, for the Ma number below the critical value, can be expressed as:

$$c_{xk} = c_f \cdot \eta_k \cdot \frac{S_{ck}}{S_k} + \Delta c_{xm} \tag{4}$$

where: c_f – drag coefficient of fuselage friction, depending upon the type of flow; η_k – coefficient allowing for the impact of fuselage thickness; η_{Ma} – coefficient allowing for compressibility; S_k – largest cross-sectional area of fuselage; S_{ck} – total fuselage surface in contact with airflow; Δc_{xm} – interference drag resulting from air intakes, which affect the fuselage.

Taking into consideration the fact that the designed imitator is characterized by not very high airspeeds, the value of the coefficient $\boldsymbol{\eta_{Ma}}$ is taken as equal to 1.

Summing up the above deliberations, the final value of the fuselage drag is obtained from the dependency 4.2 c_{xk} =0.062.

On the basis of the above values of drag coefficients for various values of the lift coefficient, it is possible to determine the polar curve of an aerial vehicle.

The drag coefficient for the whole unmanned vehicle has been calculated from:

$$c_x = \frac{c_{xs} \cdot S + c_{xk} \cdot S_k + c_{xu} \cdot S_u}{S} \cdot (1 + K_{int}) \tag{5}$$

where the interference coefficient is rather different for various aircraft, and even for different c_z.

It may be assumed that K_{int} ranges from 0.05 to 0.07. For the sake of calculations, it is assumed that K_{int}=0.05.

For c_z=1.2512, the total drag equals: c_x=0.124. On the basis of the above data, the polar curves for the whole wing and imitator were obtained.

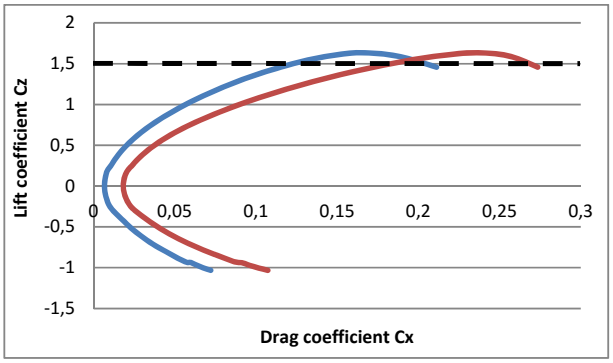

Fig. 5 Characteristics c_z=f(c_x)

VI. Section of a Propulsion System

The selection of the engine type is determined by the assumed airspeeds which an aerial vehicle is to achieve, as well as such requirements as: economy, repair and maintenance [6]. The design at stake assumes that it will be a jet engine, placed in the rear part of the fuselage, manufactured by the Safran group company - Microturbo TR-3, 300 N of thrust.

Due to lack of available characteristics of the engine, for calculations, we used a mathematical model; the thrust dependence on the Mach number has been obtained from the dependence:

$$P_r = P_{r0} \cdot \eta_{Ma} \cdot \eta_H \cdot \eta_{\bar{n}} \tag{6}$$

where: P_{r0} – engine thrust at the altitude h=0[m], in normal conditions; η_{Ma} – coefficient allowing for the influence of the Mach number; η_H – coefficient allowing for the influence of the flight altitude; $\eta_{\bar{n}}$ – coefficient allowing for the turbine rotations - $\eta_{\bar{n}} = 1$

$$\eta_{Ma} = (1 - 0{,}1Ma \cdot s_{dw}) \cdot (1 - 0{,}5Ma + 0{,}6Ma^2) \tag{7}$$

for h<11000 m

$$\eta_H = \sigma_H{}^{0{,}95-0{,}21Ma^2} \tag{8}$$

where: σ_H – ratio of air density at h altitude versus density at density h=0 m; s_{dw} – dual circuit (range) – s_{dw}=1.

VII. Determining Basic Performance

The type of a selected method in order to determine the basic performance is affected by the so-called value of thrust indicator) $\boldsymbol{q_{Pr}}$ defined as:

$$q_{Pr} = \frac{m_{to}}{P_{R-max}} \tag{9}$$

where: m_{to}=90 kg; $P_{R\text{-}max}$ =0.3 kN

Since the thrust indicator equals: q_{Pr}=300 kg/kN, in order to calculate the performance, we can use the power method [11].

The obtained dependencies enable to determine the dependencies of rate of climb and the angle of the flight path upon an altitude and a flight speed.

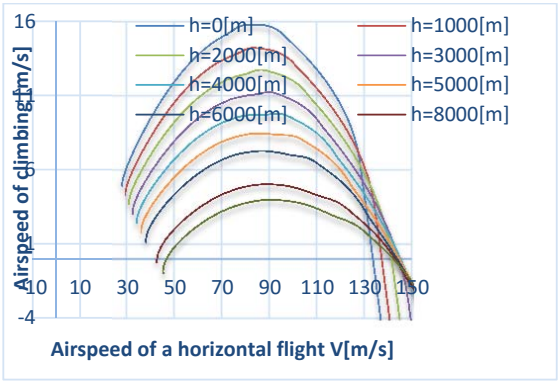

Fig. 6 Dependence of rate of climb on airspeeds for various altitudes

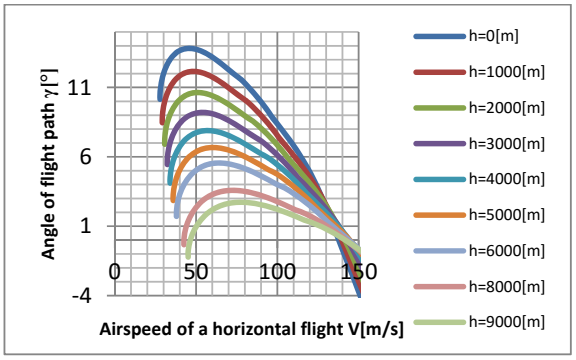

Fig. 7 Dependence between the angle of a flight path and airspeed for various altitudes

TABLE II
UAV PERFORMANCES IN RELATION TO FLIGHT ALTITUDE

h [m]	V_{min} [km/h]	V_{max} [km/h]	w_{max} [m/s]	V_w [km/h]	γ_{max} [°]	V_γ [km/h]
0	100.26	480.2	15.8	290.9	13.82	168
1000	105.25	493.2	14.22	305.3	12.15	176
2000	110.61	508.5	12.68	320.9	10.63	184.86
3000	116.38	521.28	11.1	324	9.2	194.5
4000	122.61	527	9.74	316	7.9	205
5000	129.31	528.12	8.47	317	6.67	216.14
6000	136.62	523.8	7.29	318	5.56	228.35
8000	153.44	514.8	5.04	320	3.58	256
9000	162.54	514	4	322.6	2.72	271.62

In conclusion to the above deliberations, on Fig. 8, it can be depicted basic performance of an aerial vehicle as functions of a flight altitude [10]. It also contains, apart from the previously calculated values, the service ceiling, and the absolute ceiling, which due to the limitations of the exploited engine equals 9000 m. At this altitude, the maximum rate of climb equals W_{max} = 4 m/s at the flight speed of V=322.6 km/h.

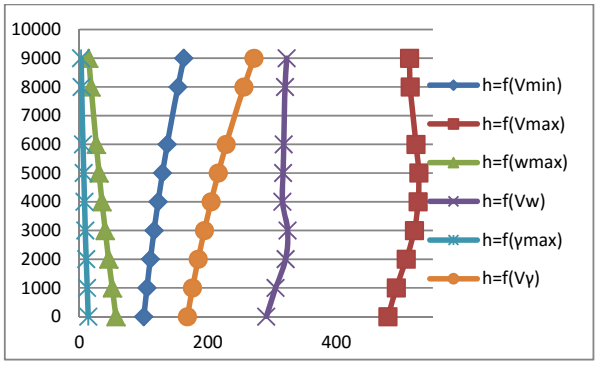

Fig. 8 Performance of the designed imitator of an aerial target

The main idea of designed imitator of an aerial target is to train the air defence personnel as well as pilots in fighting off air targets. The mission profile must meet the requirements connected with launching air defence missiles and also the requirements connected with eliminating air targets with fighter aircraft [7], [8].

The Unmanned Aerial Vehicle takes off on a launch pad. Next, the imitator of an air target, executes a task in the autonomous mode, in accordance with the programmed profile and a flight path over a designated area. The flight profile is uploaded each time before the takeoff. The flight path tracking is performed by a ground control station, which is also capable of changing the parameters during a mission. On completion of the task, a parachute set is activated for a safe landing [5].

VIII. CONCLUSION

Designing an aerial vehicle is a complex process, which covers actions that are analytical, technical, and organizational in their character. The major design work involves large teams and high financial expenditures. The costs of research and development exceed the price of one aerial vehicle by several times. Therefore, it is understandable that these stages of design which significantly influence the final output receive particular attention. Long-term experience of various companies proves that designing which is supported by extensive analysis of current needs brings about best results.

The adopted concept of the imitator of an aerial target has been shaped on the basis of a scrutiny of trends of models which are currently used. Within the project, the basic aerodynamic calculations had been made, which have enabled to determine performance and mass balance of particular components. Owing to the calculations, it was possible to bring closer the flight and technical parameters to the real performance of Unmanned Aerial Vehicles [8]. This investigation is an introduction to a design analysis over an imitator of an aerial target. Aerial vehicles of this kind are a considerable help in combat training of air units and air defense units. A low cost of the manufacture of the imitator, compared to other aerial vehicles, justifies conducting design work. Potential possibilities of exploiting imitators of aerial targets cause that its use is fully justified from the economic and military standpoint.

REFERENCES

[1] Adamski M., Rajchel J., „Bezzałogowe Statki Powietrzne, cz. I, Charakterystyka i wykorzystanie", WSOSP-Dęblin, 2013.
[2] Danielecki S., Projektowanie samolotów, Oficyna Wydawnicza Politechniki Warszawskiej, Warszawa, 2000.
[3] Fiszdon W., Mechanika lotu , PWN, Warszawa – Łódź, 1961.
[4] Grzesik N., Infrared passive homing guidance gun system on UCAV, Scientific Aspects of Unmanned Mobile Vehicle, Politechnika Świętokrzyska, Kielce, 2010.
[5] Grzegorzewski M., Ciećko A., Oszczak S., Ćwiklak J., Aircraft Landing System Utilizing a GPS Receiver with Position Prediction Capability/Functionality, ION GNSS 2011. Portland USA.
[6] Jankowska-Sieminska B., Jankowski A., Slezak M., Analysis and Research of Piston Working Conditions of Combustion Engine in High Thermal Load Conditions, Journal f KONES 2007, Vol. 14, No. 3.
[7] Jel R., Projekt wstępny imitatora celu powietrznego., Praca mgr WSOSP-Dęblin, 2010.
[8] Koruba Z., Dziopa Z., Krzysztofik I., Dynamics of a Controlled Anti-aircraft Missile Launcher Mounted on a Moveable Base, Journal of Theoretical and Applied Mechanics, Vol. 48, No. 2, 2010.
[9] Pila J., Kozuba J., Korba P., Airframe Structure, Dęblin, 2014.
[10] Warchulski J., Czechowicz B., Opracowanie projektu systemu imitatorów celów powietrznych do strzelań rakietowych ICP-SR, Warszawa, 2007.
[11] Zyluk A., Numerical simulation of the Effect of Wind on the Missile Motion, Journal of Theoretical and Applied Mechanics, 52/2, 2014.